Large-eddy simulation of multiphase flows in complex combustors

S.V. Apte[1], K. Mahesh[2], F. Ham[1], G. Constantinescu[1] & P. Moin[1]

[1] *Center for Integrated Turbulence Simulations, Stanford University, USA*
[2] *University of Minnesota, USA*

Abstract

Large-eddy simulation (LES) is a promising technique to accurately predict reacting multi-phase flows in practical combustors involving complex physical phenomena of turbulent mixing and combustion dynamics. Our goal in the present work is to develop a computational tool based on particle-tracking schemes capable of performing hi-fidelity multiphase flow simulations with models to capture liquid-sheet breakup, droplet evaporation, droplet deformation and drag. An Eulerian low-Mach number formulation on arbitrary shaped unstructured grids is used to compute the gaseous phase. The dispersed phase is solved in a Lagrangian framework by tracking a large number of particles on the unstructured grid. The interphase mass, momentum, and energy transport are modeled using two-way coupling of point-particles. A series of validation simulations are performed in coaxial and realistic gas-turbine combustor geometries to evaluate the predictions made for multiphase, turbulent flow.

1 Introduction

Turbulent multi-phase flows are encountered in a variety of engineering applications, viz., internal combustion engines, liquid and solid propellant rocket motors, gas-turbine aircraft engines, cyclone combustors and biomass gasifiers involving swirling motions. The combustion chambers of propulsion systems involve intriguing processes such as break-up and atomization of liquid fuel jets, i evaporation/condensation and collision/coalescence of droplets, turbulent mixing of fuel and oxidizer giving rise to spray-flames. Owing to the complexities of the underlying processes, accurate quantitative observations of the flowfield are formidable and often subject to large measurement errors. Better understanding of such flows

54 Computational Methods in Multiphase Flow

for design modifications, improvements, and exploring fundamental physical phenomena demands high-fidelity numerical studies in realistic configurations.

To date the engineering prediction of such flows in realistic configurations relies predominantly on the Reynolds-averaged Navier-Stokes equations (RANS). The large-eddy simulation (LES) technique has been convincingly shown to be superior to RANS in accurately predicting turbulent mixing and combustion dynamics [1] in simpler combustor geometries. Recently, Mahesh et al. [2] have developed a novel numerical algorithm for high-fidelity turbulence simulations on unstructured grids and complex geometries. This solver is extended to perform multiphase flow simulations with Lagrangian particle tracking on unstructured grids [3, 4]. The particles are treated as point-sources with two-way coupling of mass, momentum, and energy between the gas and dispersed phases.

The paper is organized as follows. Section 2 provides a brief overview of the gas and particle phase equations. The droplet evaporation and breakup models are then described. Section 3 presents results from the LES of various test cases performed in simple coaxial as well as complex realistic gas-turbine combustor geometries.

2 Theoretical formulation

The governing equations used for the gaseous and dispersed phases are briefly described.

2.1 Gas-Phase

The three-dimensional, low-Mach number, filtered Navier-Stokes equations are solved on unstructured grids with arbitrary elements. These equations are written as

$$\frac{\partial \overline{\rho_g} \tilde{u}_j}{\partial x_j} = -\frac{\partial \overline{\rho_g}}{\partial t} + \overline{\dot{S}_m} \tag{1}$$

$$\frac{\partial \overline{\rho_g} \tilde{Z}}{\partial t} + \frac{\partial \overline{\rho_g} \tilde{Z} \tilde{u}_j}{\partial x_j} = \frac{\partial}{\partial x_j} \left(\overline{\rho_g} \tilde{\alpha}_Z \frac{\partial \tilde{Z}}{\partial x_j} \right) - \frac{\partial q_{Zj}}{\partial x_j} + \overline{\dot{S}_Z} \tag{2}$$

$$\frac{\partial \overline{\rho_g} \tilde{C}}{\partial t} + \frac{\partial \overline{\rho_g} \tilde{C} \tilde{u}_j}{\partial x_j} = \frac{\partial}{\partial x_j} \left(\overline{\rho_g} \tilde{\alpha}_C \frac{\partial \tilde{C}}{\partial x_j} \right) - \frac{\partial q_{Cj}}{\partial x_j} + \overline{\dot{\omega}_C} \tag{3}$$

$$\frac{\partial \overline{\rho_g} \tilde{u}_i}{\partial t} + \frac{\partial \overline{\rho_g} \tilde{u}_i \tilde{u}_j}{\partial x_j} = -\frac{\partial \overline{p}}{\partial x_i} + \frac{\partial (2\overline{\mu} \tilde{S}_{ij})}{\partial x_j} - \frac{\partial q_{ij}}{\partial x_j} + \overline{\dot{S}_i} \tag{4}$$

$$\tilde{\rho}_g = \tilde{\rho}_g(\tilde{Z}, \tilde{C}, \tilde{Z}'') \tag{5}$$

$$\tilde{S}_{ij} = \frac{1}{2} \left(\frac{\partial \tilde{u}_i}{\partial u_j} + \frac{\partial \tilde{u}_j}{\partial u_i} \right) - \frac{1}{3} \delta_{ij} \frac{\partial \tilde{u}_k}{\partial x_k} \tag{6}$$

where the unclosed transport terms in the momentum and scalar equations are grouped into the residual stress q_{ij}, and residual scalar flux q_{Zj}, q_{Cj}. The dynamic Smagorinsky model by Moin et al. [5] is used to close these subgrid terms as demonstrated by Pierce & Moin [1]. For a two-fluid (air + fuel) mixture, one conserved scalar (the mixture fraction, Z) and a non-conserved scalar (the progress variable, C) are solved. By using the standard low-Mach number assumption and assuming unity Lewis number, the energy equation can be written as a conserved scalar transport. In addition, assuming adiabatic walls the energy equation has the same boundary condition as the mixture fraction, and the two are linearly dependent. The density is obtained from the lookup tables generated using the flamelet theory for non-premixed combustion and is dependent on the local values of the two scalars and the subgrid mixture fraction fluctuations, Z''. The source term, $\overline{\dot{\omega}_C}$, represents the reaction source term obtained from flamelet theory (Pierce & Moin [1]). The cooling effect due to evaporation of droplets (heat of vaporization) can be accounted for in the equation of state by appropriately reducing the density. The density field is then obtained as a function of the mixture fraction, fluctuations in mixture fraction, and the progress variable from lookup tables generated using the flamelet theory for non-premixed combustion [1]. The source terms in the continuity, momentum, and scalar transport equations are due to the interphase interactions.

2.2 Particle-Phase

The particle motion is simulated using the Basset-Boussinesq-Oseen (BBO) equations [6]. It is assumed that the density of the particle is much larger than that of the fluid ($\rho_p/\rho_f \sim 10^3$), particle-size is small compared to the turbulence integral length scale, and that the effect of shear on particle motion is negligible. The high value of ρ_p/ρ_f implies that the Basset force and the added mass term are small and are therefore neglected. Under these assumptions, the Lagrangian equations governing the particle motions in non-dimensional form are

$$\frac{d\mathbf{x}_p}{dt} = \mathbf{u}_p, \tag{7}$$

$$\frac{d\mathbf{u}_p}{dt} = \frac{\left(1 + aRe_p^b\right)}{\frac{1}{18}\rho_p d_p^2 Re_{ref}} \left(\mathbf{u} - \mathbf{u}_p\right) + \frac{L_{ref}}{U_{ref}^2}\mathbf{g} \tag{8}$$

where $Re_p = d_p Re_{ref}|\mathbf{u} - \mathbf{u}_p|$ is the particle Reynolds number and Re_{ref} is the reference Reynolds number based on a reference length, velocity and density $L_{ref}, U_{ref}, \rho_{ref}$, respectively. For particle Reynolds number up to 800, the constants used in the drag law are $a = 0.15, b = 0.687$ [6]. The source-term $\overline{\dot{S}_i}$ in the momentum-equations represent the 'two-way' coupling between the gas and particle-phases and is given by

$$\overline{\dot{S}_i} = -\frac{1}{V_{cv}} \sum_k \frac{\rho_p^k}{\rho_{ref}} V_p^k \frac{du_{pi}^k}{dt} \tag{9}$$

56 Computational Methods in Multiphase Flow

where the subscript p stands for the particle phase. Here, V_{cv} and $V_p^k = \frac{\pi}{6}d_p^{k^3}$ are the volumes of the computational cell and particle k, respectively. The $\sum_k$ is over all particles in a computational control volume.

The gas-phase velocity, $\mathbf{u}$, in equations (7) and (8) is computed at individual particle locations within a control volume using a generalized, tri-linear interpolation scheme for arbitrary shaped elements. Introducing higher order accurate interpolation is straight forward; however, it was found that tri-linear interpolation is sufficient to represent the gas-phase velocity field at particle locations.

2.2.1 Atomisation and breakup

Liquid spray atomization plays a crucial role in analyzing the combustion dynamics in gas-turbine combustors. In order to predict the essential global features of atomization, a stochastic model for secondary breakup that accounts for a range of product-droplet sizes is used. Specifically, for a given control volume, the characteristic radius of droplets is assumed to be a time-dependent stochastic variable with a given initial distribution function. The breakup of parent blobs into secondary droplets is viewed as the temporal and spatial evolution of this distribution function around the parent-droplet size. This distribution function follows a certain long-time behavior, which is characterized by the dominant mechanism of breakup. The size of new droplets is then sampled from the distribution function evaluated at a typical breakup time scale of the parent drop as described by Apte et al. [7]. The discrete model by Kolmogorov is reformulated in terms of a Fokker-Planck (FP) differential equation for the evolution of the size-distribution function from a parent-blob towards the log-normal law:

$$\frac{\partial T(x,t)}{\partial t} + \nu(\xi)\frac{\partial T(x,t)}{\partial x} = \frac{1}{2}\nu(\xi^2)\frac{\partial^2 T(x,t)}{\partial x^2}. \tag{10}$$

where the breakup frequency (ν) and time (t) are introduced. Here, $T(x,t)$ is the distribution function for $x = log(r_j)$, and r_j is the droplet radius. Breakup occurs when $t > t_{breakup} = 1/\nu$. The value of the breakup frequency and the critical radius of breakup are obtained by the balance between the aerodynamic and surface tension forces. The secondary droplets are sampled from the analytical solution of equation (10) corresponding to the breakup time-scale. The parameters encountered in the FP equation ($\langle \xi \rangle$ and $\langle \xi^2 \rangle$) are computed by relating them to the local Weber number for the parent blob, thereby accounting for the capillary forces and turbulent properties. As new droplets are formed, parent droplets are destroyed and Lagrangian tracking in the physical space is continued till further breakup events.

2.2.2 Hybrid approach for particle tracking

Performing spray breakup computations using Lagrangian tracking of each individual droplet gives rise to a large number of droplets (~ 50 million) very close to the injector. A hybrid scheme involving the computation of both individual droplets and parcels is used [7]. The difference between droplets and parcels is simply the number of particles associated with them, N_{par}, which is unity for
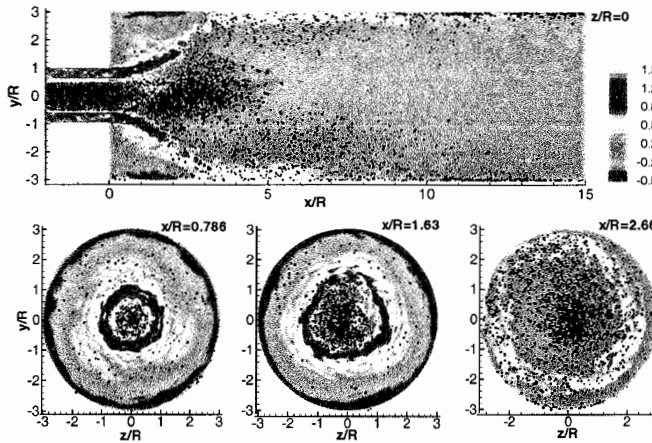
Figure 1: Snapshots of particles superposed on contours of instantaneous axial velocity at different cross-sections. Conditions correspond to the experiment by Sommerfeld & Qiu [10].

droplets. During injection, new particles added to the computational domain are pure drops ($N_{par} = 1$). These drops move downstream and undergo breakup according to the above breakup model and produce new droplets. The basic idea behind the hybrid-approach, is to collect all droplets in a particular control volume and group them into bins corresponding to their size and other properties such as velocity, temperature etc. The droplets in bins are then used to form a parcel by conserving mass, momentum, and energy. The properties of the parcel are obtained by mass-weighted averaging from individual droplets in the bin. For this procedure, only those control volumes for which the number of droplets increases above a certain threshold value are considered. The parcel thus created then undergoes breakup according to the above stochastic model, however, does not create new parcels. On the other hand, N_{par} is increased and the diameter is decreased by mass-conservation.

2.2.3 Droplet evaporation

The evaporation model is based on the single (isolated) droplet evaporation process (see e.g. Faeth [8]). The droplets are assumed to have homogeneous temperature and spherical shape. The heat and mass balance equations at the droplet surface are used to evaluate droplet temperature (T_p), evaporation rate dm_p/dt, droplet mass (m_p), and diameter (d_p). Multiplicative correction factors account for the convective effects [8]. Effects of droplet deformation, internal circulation on drag are modeled using the correlations provided by Helenbrook & Edwards [9]. Equations (7) and (8) are integrated using a fourth-order Runge-Kutta time-stepping algorithm. After obtaining the new particle positions, the particles are relocated, particles that cross interprocessor boundaries are duly transferred, boundary con-

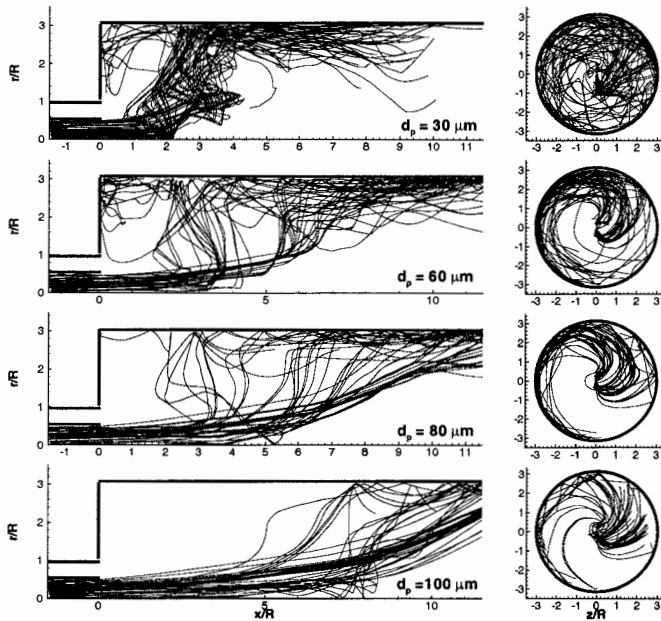58 Computational Methods in Multiphase Flow

Figure 2: Particle trajectories for different size classes.

ditions on particles crossing boundaries are applied, source terms in the gas-phase equation are computed, and the computation is further advanced.

3 Results

A systematic evaluation of the present multiphase solver is performed by performing validation simulations in coaxial and realistic combustor geometries: 1) non-reacting, particle-laden, swirling flow in a coaxial combustor [10], 2) evaporating droplets in a coaxial combustor [11], 3) spray breakup in a cylindrical Diesel engine combustion chamber, 4) atomization and breakup in a realistic gas-turbine combustor. Some salient features of these simulations are presented next. Details of some of these computations can also be found in [3, 4, 7].

3.1 Swirling particle-laden flow

Figure (1) shows the instantaneous contours of axial velocity in four different cross-sections superimposed by the scatter plot of particle positions corresponding to the experiments of Sommerfeld & Qiu [10]. A mixture of air and lightly loaded, spherical, glass-particles with a prescribed size-distribution enters the primary jet, while a swirling stream of air flows through the annulus. Good agreement with the experiment is obtained in predicting the mean and rms components of velocity for
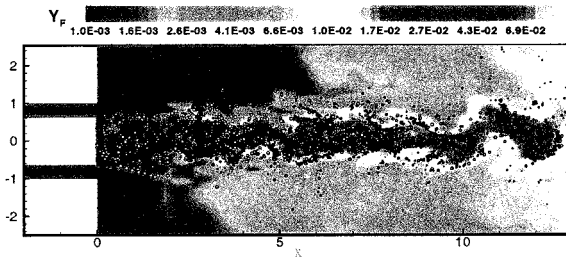
Figure 3: Snapshots of droplets superposed on contours of instantaneous fuel mass fraction. Conditions correspond to the experiment by Sommerfeld & Qiu [11].

both phases as well as the mean and rms diameter of the particles at several axial stations [4]. Each particle injected into the combustion chamber is tracked and a stationary number of approximately 1.1 million particles is obtained within the computational domain. Statistics of both phases were then collected over a couple of flow through times to obtain good results.

An in depth analysis of the particle dispersion characteristics is also performed by tracking 20,000 tagged particles of different size class. The trajectories of the different size particles are shown in Fig. (2). It is clearly seen that particles with diameters less than 80 μm decelerate to zero velocity within the central recirculation bubble. Their larger inertia causes large diameter particles to penetrate more into the recirculation zone before coming to a halt. These particles then accelerate towards the inlet and are transported radially outwards by the centrifugal forces. The particles then exit the region of reverse flow and are entrained by the annular jet which transports them downstream with swirling motion and multiple reflections off the wall. The particle residence times, size-velocity correlations obtained also show good agreement with the experimental data.

3.2 Droplet evaporation in a coaxial combustor

After obtaining good predictions of the particle-laden, swirling flow a simulation of evaporating spray in a coaxial geometry is performed corresponding to the experiments of Sommerfeld & Qiu [11]. The contours of instantaneous fuel mass fraction with scatter plot of droplets superimposed is shown in Fig. (3). Hot air (T = 373 K) is injected through the annulus. Liquid isopropyl alcohol is injected by a nozzle mounted at the center of the coaxial combustor. It forms a conical spray and the size distributions and the droplet size-velocity correlations measured at the inlet section are used as the inlet conditions. The initial temperature of the liquid is 313 K and is below its boiling point (355 K). Since, the temperature of the surrounding hot air is low, there are no reactions. Figure (4) shows the comparison of the liquid phase statistics with the experimental data. The droplet size distributions shows a typical conical spray near the injector with large size droplets accumulating on the
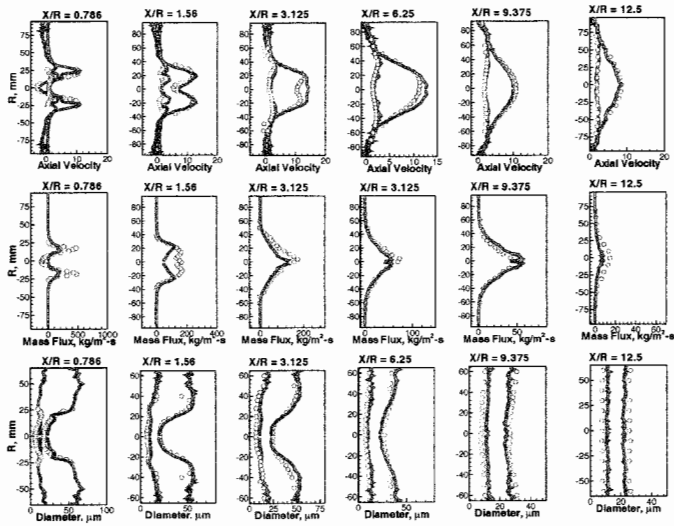
60 Computational Methods in Multiphase Flow

Figure 4: Comparison of simulation results with experimental data: mean and rms of droplet axial velocity, axial mass flux of the liquid fuel, mean and rms of droplet diameter

outer edge of the spray and small droplets in the core. These droplets evaporate and their mean diameter decreases further downstream. Predictions of the mean and rms of the axial velocity, the mean axial mass flux, and the mean and rms of droplet diameter at different axial locations are good compared to the experiments and show significant improvements over the corresponding RANS predictions.

3.3 Atomization and spray evolution in a realistic geometry

The stochastic model along with the hybrid particle-parcel approach are used to simulate spray evolution from a Pratt and Whitney injector. The experimental data set was obtained by mounting the injector in a cylindrical plenum through which air with prescribed mass-flow rate was injected. The air goes through the main and guide swirler to create a swirling jet into the atmosphere. Liquid film is injected through the filmer surface which forms an annular ring. The liquid mass-flow rate corresponds to certain operating conditions of the gas-turbine engine. Experimental data in terms of the droplet mean diameter, size distribution, and liquid mass flux in the radial direction at two different axial locations away from the injector are available. Gas-phase statistics for mean and rms velocities is also available at these locations. A snapshot of the spray evolution in the $z = 0$ plane along with the gas-phase axial velocity contours is shown in Fig.5. The hybrid-approach used herein gives a dynamical picture with correct spray angle. Results show that the liquid mass fluxes at two downstream locations are in good agreement with the
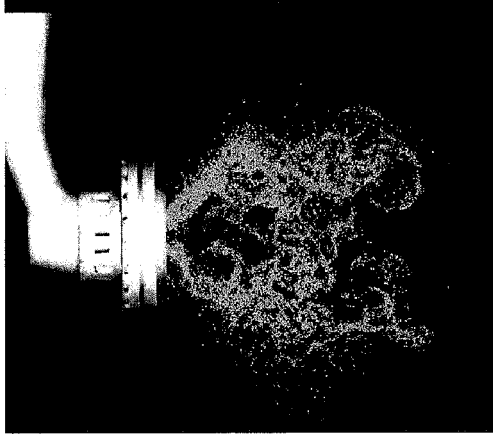
Figure 5: Instantaneous snapshot of spray evolution from a PW Injector.

experimental data. The droplet size-distribution is also in reasonable agreement considering that coalescence effects are neglected. This shows that the present solver can handle extremely complex and realistic combustor geometries. A complete computation of spray breakup, droplet evaporation, and non-premixed combustion in a real PW combustion chamber is being performed to understand the spray flame dynamics.

4 Summary

We have developed a Lagrangian Particle Tracking (LPT) framework for an unstructured grid, arbitrary shape LES solver developed by Mahesh et al. [2, 3]. The present solver can be directly used to accurately compute multi-physics, multiphase flows in realistic gas-turbine combustor geometries. The accuracy and robustness of the solver as well as its predictive capability of complex flows are verified by performing several validation studies of particle-laden, swirling flows in a coaxial combustor geometry for evaporating liquid and non-evaporating solid particles. The interphase mass, momentum, and energy exchange is modeled by two-way coupling between the phases. A stochastic model developed by Apte et al. [7] is also used to perform simulation of spray atomization in a realistic gas-turbine injector. The results obtained from these simulations are in good agreement with the available experimental data. The present solver is being extended to perform turbulent, reacting, multiphase flow simulations in complex combustor geometries.

Acknowledgements

References

[1] Pierce, C. & Moin, P., 2001, The progress variable approach for large eddy simulation of turbulent combustion, *TF-Report 80*, Flow Physics Division, Mechanical Engineering Department, Stanford University, Stanford, California.

[2] Mahesh, K., Constantinescu, G., & Moin, P., A new time-accurate finite-volume fractional-step algorithm for prediction of turbulent flows on unstructured hybrid meshes. *in preparation for Journal of Computational Physics.*, 2003.

[3] Mahesh, K., Constantinescu, G., Apte, S., Iaccarino, G., Ham, F., & Moin, P., Large-eddy simulation of gas turbines combustors. *Annual Research Briefs , Center for Turbulence Research, Stanford University*, pp. 3-17, 2002.

[4] Apte, S.V., Mahesh, K., Moin, P., & Oefelein, J.C., Large-eddy simulation of swirling particle-laden flow in a coaxial-jet combustor, *to appear in International Journal of Multiphase Flow*, 2003.

[5] Moin, P., Squires, K., Cabot, W., & Lee, S., A dynamic subgrid model for compressible turbulence and scalar transport. *Physics of Fluids. A.*, **3**, pp. 2746-2757, 1991.

[6] Crowe, C., Sommerfeld, M., & Tsuji, Y., *Multiphase flows with droplets and particles* CRC Press, Boca Raton, FL., 1998.

[7] Apte, S.V., Gorokhovski, M., & Moin, P., LES of atomizing spray with stochastic modeling of secondary breakup. *submitted for publication in International Journal of Multiphase Flow*, 2003.

[8] Faeth, G. M., Mixing, transport, and combustion in sprays. *Progress in Energy and Combustion Science*, **13**, pp. 293-345, 1987.

[9] Helenbrook, B. T., & Edwards, C. F., Quasi-steady Deformation and Drag of Uncontaminated Liquid Drops. *International Journal of Multiphase Flows*, 2002.

[10] Sommerfeld, M. & Qiu, H. H., Detailed measurements in a swirling particulate two -phase flow by a phase - doppler anemometer. *International Journal of Heat and Fluid Flow* **12(1)**, pp. 20 - 28, 1991.

[11] Sommerfeld, M. & Qiu, H. H., Experimental study of spray evaporation in turbulent flow. *International Journal of Heat and Fluid Flow* **19**, pp. 10 - 22, 1998.